polarizabilities, which have been calculated[28] for all the arenes examined here. The results are reported in Table VIII and are in general agreement with the observed relative binding energy sequence. Thus, both the inductive effects and the induced dipole effects reinforce each other, leading to the observed bond energy order.

In solution, reactions between Cr(η^6-arene)$(CO)_3$ molecules and free arenes give arene-exchange processes[8] (reaction 1), while the CO groups are displaced only under UV light irradiation.[7] The different behavior observed

$$Cr(\eta^6\text{-arene})(CO)_3 + \text{arene}' \rightleftharpoons Cr(\eta^6\text{-arene}')(CO)_3 + \text{arene} \quad (1)$$

may occur because a positive charge on the chromium atom affects the Cr–CO bond strength more than that of the Cr–arene bond, as it lowers the retro-donation contribution in the Cr–CO bond. Interestingly, the equilibrium constants of reaction 1 in solution have been reported for a number of arenes[29] and the stability of the Cr(η^6-arene)$(CO)_3$ species has been observed to increase in the order benzene, toluene, *p*-xylene, mesitylene which is in agreement with the gas-phase results.

Conclusion

The mechanisms of self-condensation and displacement processes for eight Cr(η^6-arene)$(CO)_3$ (arene = hydrocarbons, ester, and ketones) complexes have been determined by FTMS methods. Different reaction pathways have been observed for self-condensation reactions, which depend upon the nature of the coordinated arene. The extent to which substitution of the carbonyl groups and of the coordinated arene occurs has been shown to depend on the nature of both the coordinated arene ligand and the reactant arene. From CID experiments, the relative binding energy sequence of a number of arenes to Cr^+ has been obtained and correlates well with the relative stabilities of the Cr(η^6-arene)$(CO)_3$ complexes in solution.

Acknowledgment is made to the Division of Chemical Sciences in the Office of Basic Energy Sciences in the United States Department of Energy (Contract No. DE-FG02-87ER13766), to the National Science Foundation (Grant No. CHE-8920085), and to the Consiglio Nazionale delle Ricerche (Italy) for supporting this research. J.R.G. gratefully acknowledges the National Science Foundation for fellowship support.

Registry No. Cr(toluene)$(CO)_3$, 12083-24-8; Cr(mesitylene)$(CO)_3$, 12129-67-8; Cr(PhCOOMe)$(CO)_3$, 12125-87-0; Cr(PhCOMe)$(CO)_3$, 12153-11-6; Cr(PhCOEt)$(CO)_3$, 58535-55-0; Cr(PhCO-*n*-Pr)$(CO)_3$, 68786-02-7; Cr(PhCO-*t*-Bu)$(CO)_3$, 58482-51-2; Cr(PhCH$_2$COMe)$(CO)_3$, 12153-79-6; PhOMe, 100-66-3; PhCHO, 100-52-7; PhCOOMe, 93-58-3; PhCOMe, 98-86-2; PhCOEt, 93-55-0; PhCO-*n*-Pr, 495-40-9; PhCO-*t*-Bu, 938-16-9; PhCH$_2$OMe, 103-79-7; benzene, 71-43-2; propene, 115-07-1; mesitylene, 108-67-8; toluene, 108-88-3.

(28) Miller, K. J.; Savchick, J. A. *J. Am. Chem. Soc.* **1979**, *101*, 7206.
(29) Mahaffy, C. A. L.; Pauson, P. L. *J. Chem. Res., Miniprint* **1979**, 1752.

Structural Systematics. 2.[1] Metal Framework Rearrangements in Cluster Compounds Containing the Au_2Ru_3 Fragment

A. Guy Orpen*,[†] and Ian D. Salter[‡]

Department of Inorganic Chemistry, University of Bristol, Bristol BS8 1TS, U.K., and Department of Chemistry, University of Exeter, Exeter EX4 4QD, U.K.

Received March 14, 1990

It has been postulated that the reaction path for site exchange of gold atoms in cluster compounds containing Au_2Ru_3 fragments involves a partial Berry pseudorotation in which the geometry of the Au_2Ru_3 fragment changes from trigonal bipyramidal (tbp) to square pyramidal (sp) and then back to tbp with exchange of gold atom environments. This hypothesis is tested against data derived from 16 crystal structures of compounds containing such fragments. The Berry-like mechanism is shown to be fully consistent with the structural evidence. The observed geometries map the full range of the reaction coordinate. There is some evidence supporting the existence of an edge-cleavage mechanism, although only the initial stages of this pathway may be observed in the data set. Other mechanisms, such as the turnstile, are shown to be incompatible with the structural data presented.

We have shown,[2,3] in a series of studies by ^{31}P and/or ^{109}Ag NMR spectroscopy, that metal clusters containing trigonal-bipyramidal M_2Ru_3 fragments (M = Cu, Ag, Au) exhibit dynamic behavior in solution that involves intramolecular exchange between Group Ib metal atoms in axial and equatorial sites. We have further postulated[3] that this process occurs by a partial Berry pseudorotation mechanism in which the geometry of the M_2Ru_3 fragment changes from trigonal bipyramidal (tbp) to square pyramidal (sp) and then back to tbp, thereby exchanging the M atoms (see Scheme I (top), A → B → C). The integrity of the Ru_3 triangle is apparently maintained in the process, typically as a consequence of a μ_3 ligand (e.g. S, COMe, or $Ru(CO)_3$) that caps this unit. We now report that analysis of 16 crystal structures of cluster compounds

[†] University of Bristol.
[‡] University of Exeter.

(1) Part 1: Orpen, A. G.; Connelly, N. G. *Organometallics* **1990**, *9*, 1206.
(2) For example: Blaxill, C. P.; Brown, S. S. D.; Frankland, J. C.; Salter, I. D.; Sik, V. *J. Chem. Soc., Dalton Trans.* **1989**, 2039. Brown, S. S. D.; Salter, I. D.; Sik, V.; Colquhoun, I. J.; McFarlane, W.; Bates, P. A.; Hursthouse, M.; Murray, M. *J. Chem. Soc., Dalton Trans.* **1988**, 2177 and references cited therein.
(3) Farrugia, L. J.; Freeman, M. J.; Green, M.; Orpen, A. G.; Stone, F. G .A.; Salter, I. D. *J. Organomet. Chem.* **1983**, *249*, 273.

0276-7333/91/2310-0111$02.50/0

Scheme I. Berry-like Pathway Interconverting tbp Isomers A and C via the sp Isomer B (Top) and Turnstile Pathway[a] Interconverting tbp Isomers A and C via an Intermediate (A′) (Bottom)

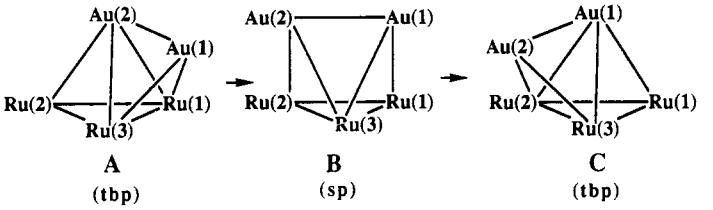

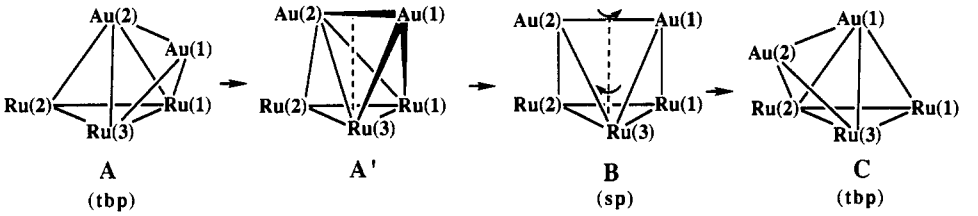

[a] In this pathway, local 2- and 3-fold axes become collinear (in A′) and the Au_2 and Ru_3 fragments rotate about these axes (indicated by the dashed line) to afford sp isomer B and eventually C.

containing the Au_2Ru_3 fragment supports this proposition and allows, for the first time, definition of a detailed picture of the pathway by which a metal cluster core rearranges.

Bürgi and Dunitz[4] have developed the application of structural data, derived from crystal structure analyses, to the study of reaction pathways. In their approach, individual molecular (or submolecular fragment) geometries are assumed to define low-energy portions of the potential energy hypersurface across which the molecule or fragment moves during reactions. In an early study of this type, Muetterties and Guggenberger showed[5] that the structures of five-coordinate phosphorus and d^8-ML_5 (M = transition metal) compounds map out the Berry pseudorotation pathway. In more recent studies of five-coordinate metal complexes, Auf der Heyde, Nassimbeni[6,7] and Bürgi[8-10] have shown, in a series of papers, that details of the Berry mechanism (and other aspects of their chemistry) may be observed by examination of the structural data for five-coordinate zinc,[6] nickel,[7] and other[8-10] (d^8) metals. We have adopted a similar approach here, applied to a topologically analogous pentametal cluster fragment.

In the language used to describe site exchange processes in boron cage chemistry, the postulated mechanism (Scheme I (top)) for Au_2Ru_3 rearrangement is termed a (single) diamond–square–diamond (dsd) mechanism. In the case of $C_2B_3H_5$, Gimarc[11] and others[12,13] have noted that the dsd mechanism is symmetry-forbidden for systems that preserve a mirror plane of symmetry. For the process in Scheme I (top), there is no such symmetry in the intermediate stages that lie between the tbp and sp geometries. Thus, the situation is analogous to the degenerate

Scheme II. Pathway Interconverting tbp Isomers A and E via the Edge-Bridged Tetrahedral Isomer D

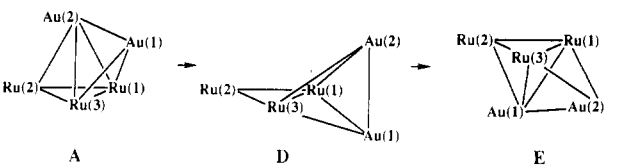

Scheme III. Pathway Interconverting tbp Isomers A and E via the Edge-Bridged Tetrahedral Isomer F, tbp Isomer G, and the Edge-Bridged Tetrahedral Isomer F′

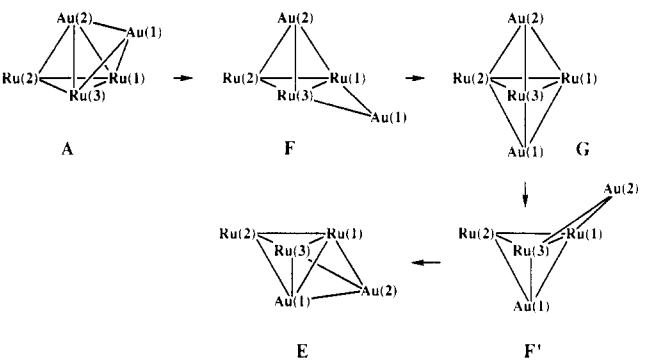

rearrangement of 1,2-$C_2B_3H_5$ in which the carbon atoms exchange sites. In neither case is there a formal symmetry barrier to rearrangement. This contrasts with the situations explicitly discussed by Gimarc and Ott[11] for nondegenerate rearrangements of 1,2-$C_2B_3H_5$ to 2,3-$C_2B_3H_5$ or 1,5-$C_2B_3H_5$, which *are* symmetry-forbidden, and are, in consequence, high-energy reactions.

The mechanisms of core atom site exchange in molecular metal cluster compounds have recently been addressed by a number of workers. During their discussions, Wales, Mingos, and Zhenyang[13] briefly touched on the behavior of gold-containing compounds and regarded them as a special case in view of the unusual bonding capabilities of $AuPR_3$ (R = alkyl, aryl) units and the weak tangential bonds formed by their gold atoms. In addition, Rodger and Johnson[14] have enumerated paths by which metal

(4) Bürgi, H. B.; Dunitz, J. D. *Acc. Chem. Res.* **1983**, *16*, 153.
(5) Muetterties, E. L.; Guggenberger, L. J. *J. Am. Soc.* **1974**, *96*, 1748.
(6) Auf der Heyde, T. P. E.; Nassimbeni, L. R. *Acta Crystallogr., Sect. B* **1984**, *40*, 582.
(7) Auf der Heyde, T. P. E.; Nassimbeni, L. R. *Inorg. Chem.* **1984**, *23*, 4525.
(8) Auf der Heyde, T. P. E.; Bürgi, H. B. *Inorg. Chem.* **1989**, *28*, 3960.
(9) Auf der Heyde, T. P. E.; Bürgi, H. B. *Inorg. Chem.* **1989**, *28*, 3970.
(10) Auf der Heyde, T. P. E.; Bürgi, H. B. *Inorg. Chem.* **1989**, *28*, 3982.
(11) Gimarc, B. M.; Ott, J. J. *Inorg. Chem.* **1986**, *25*, 83.
(12) Wales, D. J.; Stone, A. J. *Inorg. Chem.* **1987**, *26*, 3845.
(13) Wales, D. J.; Mingos, D. M. P.; Zhenyang, L. *Inorg. Chem.* **1989**, *28*, 2754. Mingos, D. M. P. *Polyhedron* **1984**, *3*, 1289.
(14) Rodger, A.; Johnson, B. F. G. *Polyhedron* **1988**, *7*, 1107.

Table I. Metal–Metal Distances (Å) within Au_2Ru_3 Fragments

compd	fragment no.	distance Au(1)–Au(2)	Au(1)–Ru(1)	Au(1)–Ru(2)	Au(1)–Ru(3)	Au(2)–Ru(1)	Au(2)–Ru(2)	Au(2)–Ru(3)	Ru(1)–Ru(2)	Ru(1)–Ru(3)	Ru(2)–Ru(3)
$[Au_3Ru_3(\mu_3\text{-COMe})(CO)_9(PPh_3)_3]$[a]	1	2.930	2.833	4.636	2.796	2.987	2.818	2.825	2.913	2.928	2.895
	2	3.010	2.844	4.694	2.807	2.987	2.825	2.818	2.928	2.913	2.895
$[Au_3Ru_4(\mu_3\text{-H})(CO)_{12}(PPh_3)_3]$[b]	3	2.834	2.822	4.720	2.840	2.972	3.008	2.838	2.967	3.006	2.979
	4	2.839	2.851	4.726	2.836	3.008	2.972	2.838	2.967	2.979	3.006
$[Au_2Ru_3(\mu_3\text{-S})(CO)_8(PPh_3)_3]$[c]	5	2.915	2.808	4.616	2.794	2.861	2.896	2.784	2.833	3.034	2.883
$[Au_2Ru_3(\mu\text{-H})(\mu_3\text{-COMe})(CO)_9(PPh_3)_2]$[c]	6	3.177	2.797	4.144	2.702	4.035	2.735	2.749	2.860	2.879	2.899
$[Au_2Ru_5W(\mu_6\text{-C})(CO)_{17}(PEt_3)_2]$[d]	7	2.808	2.865	4.652	2.839	2.907	2.935	2.886	2.936	3.109	2.957
$[Au_2Ru_3(\mu_3\text{-}C_{12}H_{15})(CO)_8(PPh_3)_3]$[e]	8	2.912	2.882	4.692	2.775	2.943	2.896	2.738	2.845	2.923	2.929
$[Au_2Ru_3(\mu_3\text{-S})(CO)_9(PPh_3)_2]$[f]	9	2.967	2.820	4.615	2.783	2.866	2.816	2.859	2.868	2.995	2.877
$[Au_2Ru_3(\mu_3\text{-C=CH}^t\text{Bu})(CO)_9(PPh_3)_2]$[g]	10	3.033	2.826	4.716	2.781	2.830	2.916	2.800	2.900	2.918	2.838
$[Au_2Ru_4(\mu_3\text{-H})(\mu\text{-H})(CO)_{12}(\mu\text{-}Ph_2PCH_2PPh_2)]$[h]	11	2.823	2.741	4.123	2.810	3.784	2.681	2.948	3.006	3.004	2.934
$[Au_2Ru_4(\mu_3\text{-H})(\mu\text{-H})(CO)_{12}(\mu\text{-}Ph_2PCH_2PPh_2)]$[h]	12	2.834	2.746	4.174	2.863	3.799	2.691	2.856	3.038	3.009	2.980
$[Au_2Ru_4(\mu_3\text{-H})(\mu\text{-H})(CO)_{12}(PPh_3)_2]$[i]	13	2.790	2.839	4.730	2.843	2.949	3.091	2.859	2.949	3.012	2.967
$[Au_2Ru_4(\mu_3\text{-H})(\mu\text{-H})(CO)_{12}(\mu\text{-}\{Ph_2PCH_2\}_2)]$[h]	14	2.828	2.784	4.444	2.777	3.446	2.851	2.965	2.984	2.946	3.008
$[Au_3Ru_4(\mu\text{-H})(CO)_{12}(\mu\text{-}Ph_2PCH_2PPh_2)\text{-}(PPh_3)]$[j]	15	2.758	2.867	4.290	2.760	3.546	2.779	2.920	2.839	2.965	3.043
	16	2.749	2.812	4.830	2.895	2.920	3.546	2.779	2.965	3.043	2.839
$[Au_2Ru_4(\mu_3\text{-H})(\mu\text{-H})(CO)_{12}(\mu\text{-}Ph_2PCHCHPPh_2)]$[k]	17	2.861	2.733	4.148	2.829	3.827	2.708	2.812	2.996	3.017	2.989
$[Au_2Ru_4(\mu_3\text{-H})(\mu\text{-H})(CO)_{12}(\mu\text{-}Ph_2AsCH_2PPh_2)]$[l]	18	2.832	2.715	4.111	2.821	3.836	2.689	2.847	3.029	3.029	2.969
$[Au_2Ru_3(\mu_3\text{-S})(CO)_9(\mu\text{-}Ph_2PCH_2PPh_2)]$[m]	19	2.802	2.785	4.321	2.792	3.335	2.742	2.836	2.773	2.968	2.923

[a] Bateman, L. W.; Green, M.; Mead, K. A.; Mills, R. M.; Salter, I. D.; Stone, F. G. A.; Woodward, P. *J. Chem. Soc., Dalton Trans.* **1983**, 2599. [b] Bruce, M. I.; Nicholson, B. K. *J. Organomet. Chem.* **1983**, *252*, 243. [c] Reference 3. [d] Bunkhall, S. R.; Holden, H. D.; Johnson, B. F. G.; Lewis, J.; Pain, G. N.; Raithby, P. R.; Taylor, M. J. *J. Chem. Soc., Chem. Commun.* **1984**, 25. [e] Bruce, M. I.; bin Shawkataly, O.; Nicholson, B. K. *J. Organomet. Chem.* **1984**, *275*, 223. [f] Bruce, M. I.; bin Shawkataly, O.; Nicholson, B. K. **1985**, *286*, 427. [g] Bruce, M. I.; Horn, E.; bin Shawkataly, O.; Snow, M. R. *J. Organomet. Chem.* **1985**, *280*, 289. [h] Reference 16a. [i] Reference 15. [j] Reference 16c. [k] Adatia, T.; McPartlin, M. Unpublished results. [l] Brown, S. S. D.; Salter, I. D.; Dyson, D. B.; Parish, R. V.; Bates, P. A.; Hursthouse, M. B. *J. Chem. Soc., Dalton Trans.* **1988**, 1795. [m] Reference 16d.

clusters might undergo site exchange on the basis of geometric criteria. They postulated that metal–metal bonds would be cleaved and formed one at a time during the rearrangement process. This postulate does not of itself lead to unambiguous prediction of mechanisms in such rearrangements, as they (and we[15]) have pointed out. In the case of an Au_2Ru_3 cluster in which the gold atoms are in contact with one another and the ruthenium atoms form a mutually bonded triangle, as in Scheme I (top), it is possible to envisage three topologically distinct pathways for gold atom site exchange (see Scheme I (top) and Schemes II and III) involving cleavage of one metal–metal bond at a time. However Schemes II and III both require that the two faces of the Ru_3 triangle be identical, but the cluster compounds studied to date invariably have a capping (μ_3) group on the face of the Ru_3 triangle not capped by the group Ib metal fragment. Thus, neither Scheme II nor Scheme III can be operative in the solution NMR studies discussed above, unless the group Ib atom site exchange is accompanied by concomitant migration of the capping (μ_3) group to the opposite side of the Ru_3 triangle. This process seems most unlikely. In addition, Scheme III is inconsistent with previous observations[2,16] that the metal frameworks of cluster compounds which contain M_2Ru_3 (M = Cu, Ag, Au) units still undergo intramolecular rearrangements in solution when the group Ib metals are linked by bidentate ligands. However, Scheme IV which is related to Scheme II, is possible in those species in which

Scheme IV. Pathway Interconverting Au_2Ru_4 Framework Isomers[a]

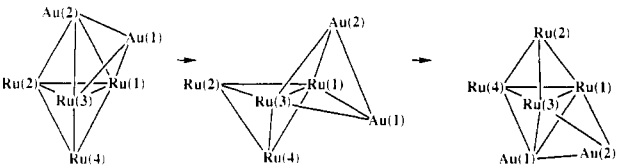

[a] Capped tbp isomers interconvert via an edge-sharing tetrahedral isomer.

the Ru_3 triangle is capped by an $Ru(CO)_3$ unit. We will not consider other mechanisms in which an edge of the Ru_3 triangle is cleaved, because these seem very unlikely given the constraints of the capping ligands.

Theoretical[17] and experimental[18] studies of related dynamic processes have suggested that site exchange in five-coordinate phosphorus species PR_5 occurs by the Berry pseudorotation rather than the turnstile[19] mechanism. In the turnstile mechanism, as originally suggested for the PR_5 system, two substituents rotate about the local 2-fold axis bisecting them while the other three rotate about the local 3-fold axis passing through their centroid. During the process, these local axes are postulated to be collinear and to pass through the phosphorus atom. An analogous process for the Au_2Ru_3 fragment is illustrated in Scheme I (bottom).

(15) Freeman, M. J.; Orpen, A. G.; Salter, I. D. *J. Chem. Soc., Dalton Trans.* **1987**, 379.

(16) For example: (a) Brown, S. S. D.; Salter, I. D.; Dent, A. J.; Kitchen, G. F. M.; Orpen, A. G.; Bates, P. A.; Hursthouse, M. B. *J. Chem. Soc., Dalton Trans.* **1989**, 1227. (b) Brown, S. S. D.; McCarthy, P. J.; Salter, I. D.; Bates, P. A.; Hursthouse, M.; Colquhoun, I. J.; McFarlane, W.; Murray, M. *J. Chem. Soc., Dalton Trans.* **1988**, 2787. (c) Adatia, T.; McPartlin, M.; Salter, I. D.; *J. Chem. Soc., Dalton Trans.* **1988**, 751. (d) Brown, S. S. D.; Hudson, S.; McPartlin, M.; Salter, I. D. *J. Chem. Soc., Dalton Trans.* **1987**, 1967 and references cited therein.

(17) Hoffmann, R.; Howell, J. M.; Muetterties, E. L. *J. Am. Chem. Soc.* **1972**, *94*, 3047. Altmann, J. A.; Yates, K.; Csizmadia, I. G. *J. Am. Chem. Soc.* **1976**, *98*, 1450. Strich, A. *Inorg. Chem.* **1978**, *17*, 942. Wang, P.; Agrafiotis, D. K.; Streitweiser, A.; Schleyer, P. v. R. *J. Chem. Soc., Chem. Commun.* **1990**, 201.

(18) Holmes, R. R. *Acc. Chem. Res.* **1979**, *12*, 257. Day, R. O.; Holmes, J. M.; Shafieezad, S.; Chandresekar, V.; Holmes, R. R. *J. Am. Chem. Soc.* **1988**, *110*, 5377.

(19) Ugi, I.; Marquarding, D.; Klusacek, H.; Gillespie, P.; Ramirez, F. *Acc. Chem. Res.* **1971**, *4*, 288.

Chart I. Labeling Scheme for Angles (θ_{ij}) Subtended at the Cluster Centroid and Dihedral Angles (Δ_{ij}) between Faces of the Cluster Polyhedron[a]

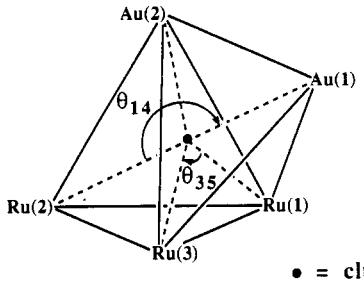

• = cluster centroid

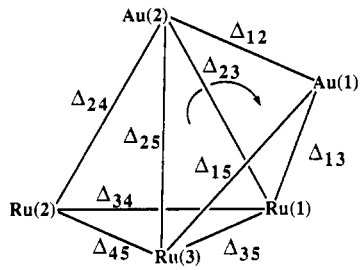

[a] Δ_{ij}'s are given at edges common to the two faces. θ_{ij}'s are numbered so that i and j refer to metal atoms Au(1), Au(2), Ru(2), Ru(2), and Ru(3) as i,j = 1, 2, 3, 4, and 5, respectively.

Our intention in this paper is to evaluate the various suggested mechanisms for site exchange in five-metal-atom cluster compounds and related systems as outlined above. We will be taking the view that the proposed mechanisms should be in accord with the structural data in that they only involve metal atom geometries which are close to those observed in the solid-state structures of clusters containing the Au_2Ru_3 fragment. This test of theory is, therefore, based on the structure correlation principle outlined and developed by Bürgi and Dunitz.[4]

Results and Discussion

In Table I, we list the metal–metal distances within 19 Au_2Ru_3 fragments derived from 16 crystal structure analyses. The atomic numbering scheme is shown for A and B in Scheme I (top) and is chosen such that the lengths Au(1)–Ru(2) > Au(2)–Ru(1) > Au(2)–Ru(3), thereby uniquely defining the metal atom labels. The geometries of the Au_2Ru_3 fragments were variously described as tbp, sp, or distorted versions thereof in the original publications of these structures. While a number of approaches may be used to quantify the degree of distortion from ideal tbp or sp geometry, we have chosen to focus primarily on the metal–metal interatomic distances, since they relate directly to the bond cleavage and formation processes of interest to chemists, and on the dihedral angles between the external faces of the metal polyhedron, as used by many workers to describe five-coordinate geometries in PR_5 and ML_5 chemistry.[5-7,18] In addition to these parameters, the angles subtended by the metal atoms at the centroid of the Au_2Ru_3 fragment (defined by the arithmetic mean of the five atomic positions) were calculated. The nomenclature for these parameters, Δ_{ij} and θ_{ij}, is illustrated in Chart I.

The partial Berry pseudorotation mechanism for the site exchange between axial and equatorial gold atom sites (Scheme I (top)) involves cleavage of the Au(2)–Ru(1) bond present in A followed by formation of the Au(1)–Ru(2) bond in C, with the Au(2)–Ru(1) and Au(1)–Ru(2) distances in B being approximately equal. C is equivalent to A, with permuted atom labels, and therefore, we may generate an additional 19 fragment geometries of type C from those in Table I. With the original structures, these give the 38 points shown in Figures 1 and 2;[20] they reveal the full range of the geometry variations that link one tbp (A) with another (C) via the sp form B. Plots with just the unique set of 19 points show how tbp fragments are deformed to give sp and other intermediate geometries. An additional but equivalent pathway leading to full exchange of ruthenium as well as gold sites in A may be readily constructed from the A → B → C pathway. Thus, cleavage of the Au(2)–Ru(3) bond in A rather than Au(2)–Ru(1) leads to another sp form equivalent to B, and closure of the Au(1)–Ru(2) distance will give another tbp form equivalent to C, but with ruthenium atom sites permuted.

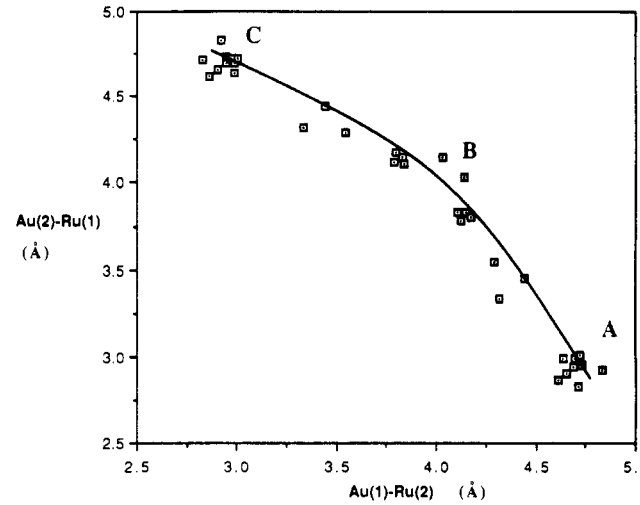

Figure 1. Selected Au–Ru distances (Å) for the 19 Au_2Ru_3 fragments, labeled as in A and listed in Table I, and 19 others generated by relabeling as in C. Au(2)–Ru(1) is plotted against Au(1)–Ru(2). Qualitative correlation paths are drawn for guidance through individual points, and the approximate locations of A–C are indicated.

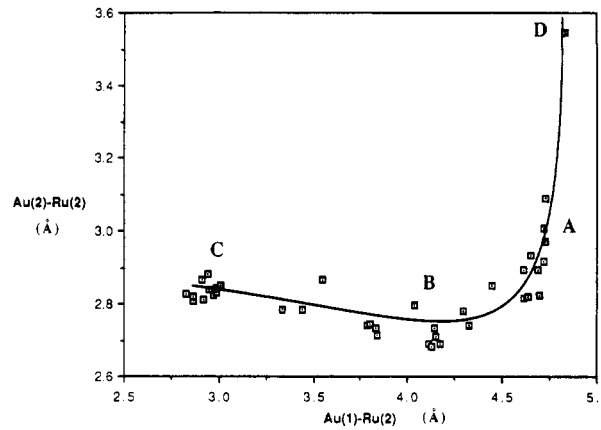

Figure 2. Selected Au–Ru distances (Å) for the 19 Au_2Ru_3 fragments, labeled as in A and listed in Table I, and 19 others generated by relabeling as in C. Au(2)–Ru(2) is plotted against Au(1)–Ru(2). Qualitative correlation paths are drawn for guidance through individual points, and the approximate locations of A–D are indicated.

(20) Auf der Heyde and Bürgi[8-10] have discussed in detail the symmetry permutations possible for the topologically identical ML_5 pathways. We note here that the symmetries of the ideal tbp and sp in the Au_2Ru_3 clusters are both C_s rather than D_{3h} and C_{4v} as in the ML_5 situation and that the symmetry of the intermediate structures is only C_1.

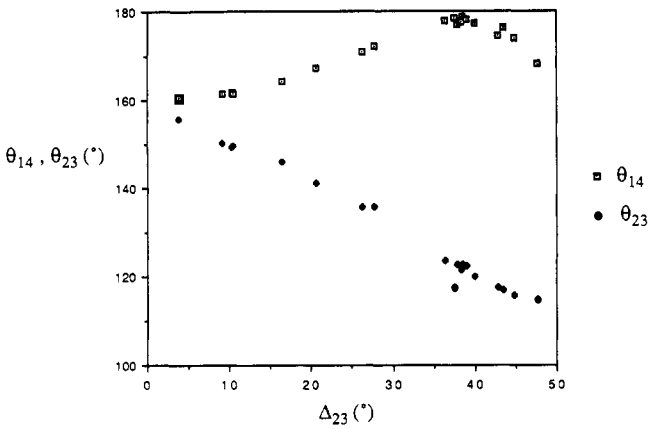

Figure 3. Angles subtended at the centroid of the Au_2Ru_3 cluster (θ_{14} and θ_{23}) plotted against the dihedral angle between the Au(1)Au(2)Ru(1) and Au(2)Ru(1)Ru(2) planes (Δ_{23}).

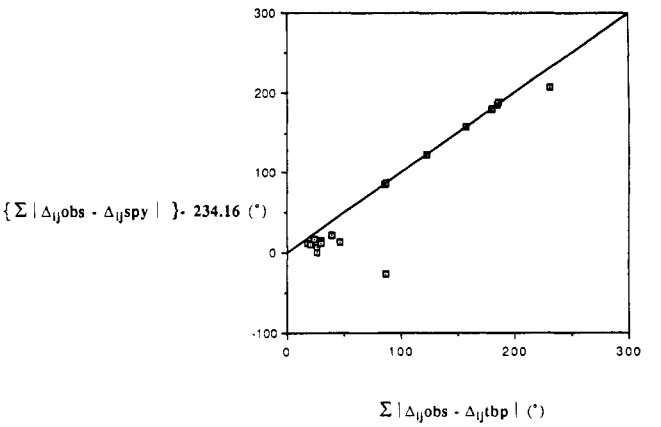

Figure 4. Sums of absolute differences between observed dihedral angles (Δ_{ij}) for the Au_2Ru_3 polyhedra and idealized values for tbp and sp geometries.[22]

The correlation between the various Au–Ru distances during the rearrangement process A → C is clearly revealed by plotting Au(2)–Ru(1) against Au(1)–Ru(2) (Figure 1). The smooth, curvilinear relationship between these parameters suggests that they might serve as the basis for a reaction coordinate, a point that we shall return to in due course.

Although many of the structures in Table I are closely grouped with Au(1)–Ru(2) = ca. 4.7 Å and Au(2)–Ru(1) = ca. 2.85 Å, i.e. with a tbp geometry, there exists a series of points spanning the full range of geometries through tbp to sp and back to tbp again. As shown in Figure 1, the correlation between Au(1)–Ru(2) and Au(2)–Ru(1) shows pronounced nonlinearity. At the midpoint of the reaction coordinate (B), the sum of the two Au–Ru distances is ca. 8.0 Å, and at the endpoints (tbp), it is ca. 7.5 Å. Although nonlinearity in similar plots of interatomic distances for bond formation and cleavage processes have previously been observed,[4] the curvature has typically been in the opposite sense, with the sum of lengths reduced at the midpoint of the reaction. This latter behavior has been viewed as a consequence of the conservation of bond order, long postulated[21] as an important factor in determining chemical reaction pathways. Figure 2 shows a second aspect of the correlated deformations in the cluster geometries present in these compounds. Thus, Au(2)–Ru(2) falls from ca. 2.9 Å in A to ca. 2.72 Å at the reaction midpoint B before rising against in C. This might imply some strengthening of the Au(2)–Ru(2) (and so also Au(1)–Ru(1)) bonds in B relative to those in A or C, which compensates for the net weakening of the Au(1)–Ru(2) and Au(2)–Ru(1) bonds revealed by Figure 1. In A, which lies at the terminus of the Berry-type reaction coordinate, there is clear evidence of a tendency to lengthening of the Au(2)–Ru(2) distance (see Figure 2). Further extension and cleavage of this bond forms D, an edge-bridged tetrahedral geometry (in which Au(2)–Ru(2) is equal in length to Au(1)–Ru(2)), which is an intermediate on the pathway of Scheme II. As discussed above, it is extremely unlikely that Scheme II operates in solution for any of the clusters containing M_2Ru_3 (M = Cu, Ag, or Au) units that have been studied by NMR spectroscopy to date, but it remains an intriguing possibility. In addition, the closely related Scheme IV is consistent with NMR spectroscopic data for clusters with capped-trigonal-bipyramidal M_2Ru_4 metal frameworks.[15]

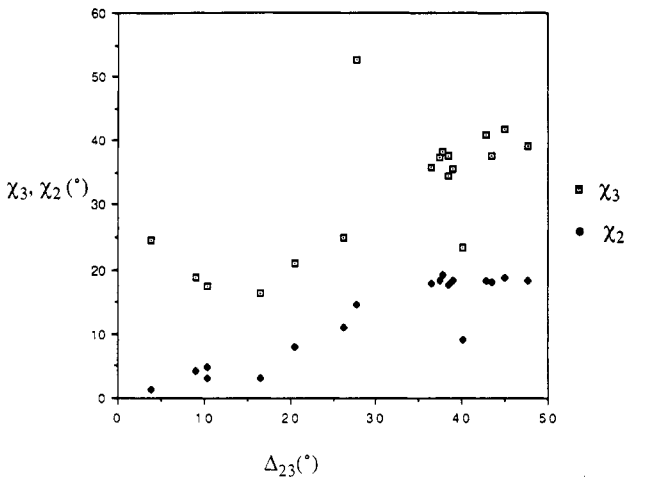

Figure 5. Variation of angles χ_2 and χ_3 as a function of Δ_{23}.

While the trajectory illustrated in Figure 1 is consistent with a Berry-like mechanism, more rigorous tests of the details of this hypothesis are possible. Several groups have used the dihedral angles between the faces of the polyhedron formed by the ligands in five-coordinate complexes as a powerful tool for describing their geometry. The angles subtended at the central atom in such species have also been used to characterize their coordination geometry. In the case studied here, there is, of course, no central atom and analogous angles were therefore calculated about the centroid of the five metal atoms. A plot of Δ_{23} against θ_{14} and θ_{23} is shown in Figure 3. Its form is strongly reminiscent of that of an analogous plot for PR_5 and SnL_5 species given by Holmes[18] and by other authors[5-7] for ML_5 species. Furthermore, plotting the summed magnitudes of the deviations of dihedral angles from idealized tbp and sp values gives the characteristic linear unit-slope graph illustrated in Figure 4. Again, this is very similar to such plots for PR_5[18] and ML_5[5-7] species. Here we have assumed the idealized tbp and sp to have equilateral triangular faces (of length 2.9 Å) and the sp to have $\theta_{14} = \theta_{23} = 160°$, as suggested by Figure 3.[22] The points furthest from the ideal line in Figure 4 correspond to the fragments (notably number 16) in Table I in which the tbp is distorted toward form D. The plots in Figures 3 and 4 are, therefore, fully consistent with a Berry-like mechanism (Scheme I (top)).

(21) See discussion in: Dunitz, J. D. *X-Ray Analysis and the Structure of Organic Molecules*; Cornell University Press: Ithaca, NY, 1979; Chapter 7.

(22) Calculated dihedral angles (deg) for ideal tbp (and sp) are as follows: Δ_{12}, 109.5 (125.3); Δ_{13}, 109.5 (125.3); Δ_{15}, 109.5 (70.5); Δ_{23}, 38.9 (0.0); Δ_{24}, 109.5 (125.3); Δ_{25}, 38.9 (70.5); Δ_{34}, 109.5 (125.3); Δ_{35}, 38.9 (70.5); Δ_{45}, 109.5 (70.5).

Table II. Principal Component Analysis of Metal–Metal Distances in 38 Au_2Ru_3 Cluster Fragments

Covariance Matrix

	Au1Au2	Au1Ru1	Au1Ru2	Au2Ru1	Au2Ru2	Au1Ru3	Au2Ru3	Ru1Ru2	Ru1Ru3	Ru2Ru3
Au1Au2	0.011									
Au1Ru1	−0.003	0.022								
Au1Ru2	0.001	−0.041	0.512							
Au2Ru1	0.001	0.032	−0.494	0.512						
Au2Ru2	−0.003	0.003	0.032	−0.041	0.022					
Au1Ru3	−0.003	−0.001	−0.007	0.007	0.001	0.003				
Au2Ru3	−0.003	0.001	0.007	−0.007	−0.001	−0.000	0.003			
Ru1Ru2	−0.002	−0.001	0.003	0.003	−0.001	0.002	0.002	0.005		
Ru1Ru3	−0.003	−0.003	0.020	−0.019	0.002	0.001	0.001	0.001	0.004	
Ru2Ru3	−0.003	0.002	−0.019	0.020	−0.003	0.001	0.001	0.001	0.000	0.004

Latent Roots (Eigenvalues)

1	2	3	4	5	6	7	8	9	10
1.013	0.032	0.018	0.015	0.011	0.003	0.002	0.002	0.001	0.001

Composition of Principal Components

	component					component			
	1	2	3	4		1	2	3	4
Au1Au2	0.000	0.032	−0.090	0.000	Au1Ru3	0.010	−0.004	0.031	−0.024
Au1Ru1	0.052	−0.101	0.014	0.081	Au2Ru3	−0.010	−0.004	0.031	0.024
Au1Ru2	−0.709	0.070	0.035	0.006	Ru1Ru2	0.000	0.018	0.049	−0.000
Au2Ru1	0.709	0.070	0.035	−0.006	Ru1Ru3	−0.027	0.002	0.035	−0.016
Au2Ru2	−0.052	−0.101	0.014	−0.081	Ru2Ru3	0.027	0.002	0.035	0.016

Percent of Total Variance Explained by Components

component			
1	2	3	4
92.334	2.874	1.617	1.371

Table III. Pearson Correlation Matrix for 19 Sets of Metal–Metal Distances in the Au_2Ru_3 Fragments Listed in Table I

	Au1Au2	Au1Ru1	Au1Ru2	Au2Ru1	Au2Ru2	Au1Ru3	Au2Ru3	Ru1Ru2	Ru1Ru3	Ru2Ru3
Au1Au2	1.000									
Au1Ru1	0.080	1.000								
Au1Ru2	−0.021	0.746	1.000							
Au2Ru1	0.043	−0.719	−0.957	1.000						
Au2Ru2	−0.299	0.410	0.740	−0.604	1.000					
Au1Ru3	−0.661	−0.151	0.293	−0.246	0.526	1.000				
Au2Ru3	−0.518	−0.140	−0.241	0.179	−0.235	0.118	1.000			
Ru1Ru2	−0.300	−0.518	−0.198	0.320	0.038	0.604	0.338	1.000		
Ru1Ru3	−0.668	−0.194	0.038	−0.110	0.277	0.704	0.357	0.363	1.000	
Ru2Ru3	−0.511	−0.088	−0.378	0.417	−0.333	0.067	0.549	0.322	0.184	1.000

The turnstile mechanism (Scheme I (bottom)) may be rejected on the basis of the evidence illustrated in Figure 5. This shows the variations of χ_2 and χ_3 as a function of Δ_{23}. χ_2 is defined as the deviation of the local 2-fold axis (which perpendicularly bisects the Au–Au vector and passes through the centroid of the Au_2Ru_3 cluster) from collinearity with the line from the midpoint of the Au–Au vector to the centroid of the Au_2Ru_3 cluster. χ_3 is defined as the deviation of the local 3-fold axis (the perpendicular to the Ru_3 triangle) from collinearity with the line from the centroid of the Ru_3 triangle to the centroid of the Au_2Ru_3 cluster. In Figure 5, Δ_{23} acts as a measure of the distortion from tbp (at the right-hand extremity of the plot where $\Delta_{23} \approx 40$–$45°$) to sp (where $\Delta_{23} = 0°$). In the turnstile mechanism χ_2 and χ_3 are supposed to fall to zero early in the pathway as the two axes become collinear. This does not happen in the structures examined here, as χ_3 never falls below 15° and χ_2 only reaches 0° at the sp geometry (as it must by definition).

Bürgi has suggested[23] the use of principal component analysis (pca) as an unbiased way to derive a reaction coordinate from structural data. Application[24] of pca to the covariance matrix of the symmetry-expanded set of metal–metal bond lengths (i.e. for 38 Au_2Ru_3 fragments) presented herein leads to the results of Table II. The first principal component, which explains over 92% of the variance in the data set of the 10 metal–metal distances within each of the 38 Au_2Ru_3 fragments, is composed almost entirely of the difference between the Au(1)–Ru(2) and Au(2)–Ru(1) distances. Therefore, this component may be viewed as describing the position of a fragment on the curve drawn in Figure 1 and its predominance suggests that Δ = [Au(1)–Ru(2) − Au(2)–Ru(1)] is a suitable reaction coordinate for the rearrangement mapped by the data in Table I. The equivalence of this reaction coordinate with Δ_{23}, used in Figures 3 and 5, is indicated by the high linear correlation between Δ and Δ_{23} (Pearson correlation coefficient 0.98).

As is necessarily the case, given the results of the pca above, other changes in metal–metal distances during the A → B → C rearrangement are relatively small. There are, however, a number of trends within these data. Table III lists the Pearson correlation matrix for the 19 unique sets of metal–metal distances of Table I, i.e. those for fragments

(23) Bürgi, H.-B.; Dubler-Steudle, K. C. *J. Am. Chem. Soc.* **1988**, *110*, 4953. Bürgi, H.-B.; Dubler-Steudle, K. C. *J. Am. Chem. Soc.* **1988**, *110*, 7291.

(24) See e.g.: Chatfield, C.; Collins, A. J. *Introduction to Multivariate Analysis*; Chapman and Hall: London, 1980. FASTAT 1.0, Systat Inc., Evanston, IL, 1989.

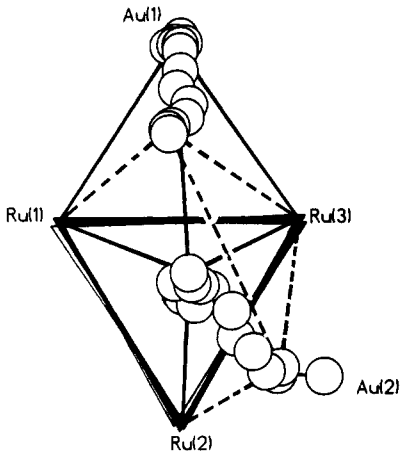

Figure 6. Trajectory of the gold atoms during the process A → B. Ru_3 triangles are superimposed for the 19 geometries of Table I; example tbp and sp (dashed) frameworks are shown.

which have geometries that lie between A and B. The most outstanding feature is the high linear correlation (coefficient −0.96) that exists between Au(1)–Ru(2) and Au(2)–Ru(1), as is to be expected given the appearance of Figure 1. The next largest correlations involve the Au(1)–Ru(1) and Au(2)–Ru(2) distances, which correlate strongly (coefficients with magnitudes between 0.6 and 0.75) with the Au(1)–Ru(2) and Au(2)–Ru(1) distances. These are the relationships illustrated in Figure 2. When the signs of the correlation coefficients are taken into account, they indicate a strong tendency for the Au(1)–Ru(1) and Au(2)–Ru(2) distances to decrease on going from A to B, i.e. from tbp to sp, as discussed above (see discussion of Figure 2). Other correlations are perhaps less predictable. For example, while the Au–Au distance is apparently *not* correlated to the distances that are indicators for the reaction coordinate (Au(1)–Ru(2) and Au(2)–Ru(1)), it is negatively correlated to all of the Ru(3)–Au and Ru–Ru distances. The implication is that increased Au–Au interaction (as reflected in the shortened Au–Au distance) is accompanied by reduced Ru(3)–Au and Ru–Ru bonding. The positive correlation of the Au(1)–Ru(3) distance with the Ru(1)–Ru(2) and Ru(1)–Ru(3) distances (coefficients 0.60 and 0.70, respectively) is likewise unexpected, but it may be in part a consequence of the increased Au(1)–Ru(1) interaction on progressing from A to B, leading to reduced Ru(1)–other metal bonding. On a cautionary note, however, it is clear that these correlation coefficients are derived from a relatively small body of data and, therefore, these observations must be reviewed as preliminary.

The trajectories of the gold atoms during the reaction pathway mapped by the structures studied here are shown in Figure 6. The Ru_3 triangles have been superimposed by least-squares fits, and the gold atom positions are illustrated for each of the 19 fragments; representative tbp and sp frameworks are shown (the latter as dashed lines).

Acknowledgment. We thank the many chemists and crystallographers who synthesized and determined the structures of the molecules listed in Table I.

Registry No. $Au_2Ru_4(\mu_3\text{-}H)(\mu\text{-}H)(CO)_{12}(\mu\text{-}Ph_2PCHCHPPh_2)$, 130063-55-7.